Published in final edited form as:
Brain Res. 2008 May 1; 1207: 84–95. doi:10.1016/j.brainres.2008.02.036.

TOTAL NUMBER, DISTRIBUTION, AND PHENOTYPE OF CELLS EXPRESSING CHONDROITIN SULPHATE PROTEOGLYCANS IN THE NORMAL HUMAN AMYGDALA

Harry Pantazopoulos, A.L.M[1], **Elisabeth A. Murray, Ph.D.**[2], and **Sabina Berretta, M.D.**[1,3]

1 *Translational Neuroscience Laboratory, Mclean Hospital, Belmont, MA, USA*

2 *Laboratory of Neuropsychology, National Institute of Mental Health, NIH, Bethesda, MD 20892, USA*

3 *Department of Psychiatry, Harvard Med. School, Boston, MA, USA*

Abstract

Chondroitin sulphate proteoglycans (CSPGs) are a key structural component of the brain extracellular matrix. They are involved in critical neurodevelopmental functions and are one of the main components of pericellular aggregates known as perineuronal nets. As a step toward investigating their functional and pathophysiological roles in the human amygdala, we assessed the pattern of CSPG expression in the normal human amygdala using *wisteria floribunda agglutinin* (WFA) lectin-histochemistry. Total numbers of WFA-labeled elements were measured in the lateral (LN), basal (BN), accessory basal (ABN) and cortical (CO) nuclei of the amygdala from 15 normal adult human subjects. For interspecies qualitative comparison, we also investigated the pattern of WFA labeling in the amygdala of naïve rats (n=32) and rhesus monkeys (Macaca mulatta; n=6). In human amygdala, WFA lectin-histochemistry resulted in labeling of perineuronal nets and cells with clear glial morphology, while neurons did not show WFA-labeling. Total numbers of WFA-labeled glial cells showed high interindividual variability. These cells aggregated in clusters with a consistent between-subjects spatial distribution. In a subset of human subjects (n=5), dual color fluorescence using an antibody raised against glial fibrillary acidic protein (GFAP) and WFA showed that the majority (93.7%) of WFA-labeled glial cells correspond to astrocytes. In rat and monkey amygdala, WFA histochemistry labeled perineuronal nets, but not glial cells. These results suggest that astrocytes are the main cell type expressing CSPGs in the adult human amygdala. Their highly segregated distribution pattern suggests that these cells serve specialized functions within human amygdalar nuclei.

Keywords

astrocyte; perineuronal net; glial fibrillary acidic protein; dual fluorescence microscopy; postmortem; wisteria floribunda agglutinin

Corresponding Author: Sabina Berretta, M.D., McLean Hospital, 115 Mill Street, Belmont MA 02478, Phone: (617) 855-3484, Fax: (617) 855-3850, E-mail: s.berretta@mclean.harvard.edu.

2. INTRODUCTION

The adult brain extracellular matrix (ECM) is mainly composed of hyaluronic acid, glycoproteins, and chondroitin sulfate proteoglycans (CSPGs) predominantly belonging to the lectican family (Ruoslahti, 1996, Viapiano, et al., 2006, Yamaguchi, 2000). During development, the CSPG spatio-temporal expression is tightly regulated, as these molecules are involved in processes such as cell differentiation and migration, axon growth and guidance. (Bandtlow, et al., 2000, Bovolenta, et al., 2000, Hartmann, et al., 2001, Kinsella, et al., 2004, Zacharias, et al., 2006). In the adult brain, CSPGs have been shown to interact with cell surface molecules, neurotrophic factors, neuronal ion channels, as well as glutamate and GABA receptors and are thought to affect plastic phenomena including long term potentiation (Bandtlow, et al., 2000, Brakebusch, et al., 2002, Bukalo, et al., 2001, Corvetti, et al., 2005, Dityatev, et al., 2003, Dityatev, et al., 2006, Okamoto, et al., 1994, Rauch, et al., 2001, Rhodes, et al., 2004, Smith, et al., 2005, Zhou, et al., 2001). Ternary complexes composed of CSPGs, hyaluronic acid, and glycoproteins are the main components of pericellular aggregates known as perineuronal nets (Celio, et al., 1998, Deepa, et al., 2006, Yamaguchi, 2000). These nets are dense, mesh-like ‘gloves’ found to surround the soma, primary dendrites and initial axonal segment of distinct neuronal populations, the most well-studied of which is a group of fast-spiking neurons expressing the calcium binding protein parvalbumin (Berghuis, et al., 2004, Bruckner, et al., 2006, Hartig, et al., 1994, Morris, et al., 2000, Pantazopoulos, et al., 2006). Current evidence suggests that perineuronal nets form gradually around successful synaptic connections and may restrict further changes of those synapses (Dityatev, et al., 2003). Together, these findings support the idea that CSPGs play a broad range of key roles in the developing and adult brain, including modulation of structural and functional plasticity.

CSPGs are composed of a core protein and a glycosaminoglycan moiety consisting of a variable number of chondroitin sulfate chains (Ruoslahti, 1996). The lectin *wisteria floribunda agglutinin*, as well as other plant-derived lectins, binds to the N-acetyl-galactosamine component of the chondroitin sulfate chains and represents a useful tool to detect CSPGs in brain tissue (Bruckner, et al., 1993, Celio, et al., 1998, Hartig, et al., 1994, Hartig, et al., 1992, Nakagawa, et al., 1986, Pantazopoulos, et al., 2006). In adult rodents, CSPGs secreted in the ECM, and associated with perineuronal nets, are synthesized and expressed by several different cell types, including neurons, astrocytes, oligodendrocytes and NG2-expressing oligodendrocyte precursor cells (Carulli, et al., 2006, Hamel, et al., 2005, John, et al., 2006, McKeon, et al., 1999, Thon, et al., 2000, Viapiano, et al., 2006).

Emerging evidence points to a role for CSPGs in the pathophysiology of several neurological disorders, including Alzheimer’s disease, multiple sclerosis and temporal lobe epilepsy (Perosa, et al., 2002, Sobel, et al., 2001, Viapiano, et al., 2006). Their role in neural injuries has also been extensively investigated, as some CSPGs inhibit neurite regeneration following neural injuries (McKeon, et al., 1991, Morgenstern, et al., 2002, Viapiano, et al., 2006). The involvement of CSPGs in the pathogenesis of psychiatric illnesses has not been investigated systematically thus far. Preliminary results from our laboratory strongly suggest that these molecules may be altered in temporal lobe regions of subjects with schizophrenia (Pantazopolous, et al., 2006). We note that CSPG functions may bear direct relevance to the pathophysiology of this disease. For instance, in schizophrenic subjects, disruptions of cell migration and abnormal numbers of axon fibers, suggestive of a disruption of axonal guidance, may be related to altered CSPG expression (Akbarian, et al., 1996, Arnold, et al., 1991, Falkai, et al., 2000, Jakob, et al., 1986, Jakob, et al., 1994, Kovalenko, et al., 2003, Longson, et al., 1996). Direct functional interactions between neurotransmitters known to be involved in this disorder, such as glutamate and GABA, and CSPGs have been described by several authors (Dityatev, et al., 2007, Schwarzacher, et al., 2006). Finally, several other extracellular matrix components, notably reelin, and interacting molecules such as neuregulin 1, neural cell

adhesion molecules and semaphorin 3A, have been found to be abnormal in schizophrenia (Corfas, et al., 2004, Costa, et al., 2004, Dong, et al., 2005, Eastwood, et al., 2003, Guidotti, et al., 2000, Guidotti, et al., 2000, Hahn, et al., 2006, Harrison, et al., 2006, Vawter, et al., 2000, Vawter, et al., 2001).

Despite their relevance to human diseases, little information is currently available regarding the distribution and phenotype of cells expressing CSPGs in the adult human brain. As a first step toward investigating the role of these molecules in psychiatric illnesses involving the amygdala, we characterized the distribution and measured total numbers of WFA-labeled cells, putatively expressing CSPGs, in the lateral (LN), basal (BN), accessory basal (ABN) and cortical (CO) nuclei of the amygdala of healthy human subjects. This group of amygdala nuclei will be from here on referred to as BLC-CO. The central nucleus of the amygdala was not included in this analysis because tissue blocks did not consistently include this nucleus in its entirety. Dual labeling fluorescent microscopy was then used to determine whether WFA-labeled cells correspond to astrocytes. Patterns of CSPG expression in the amygdala of naïve rats and rhesus monkeys (*Macaca mulatta*) were examined, and compared qualitatively to those characterized in human, in order to test for species generality.

3. RESULTS

WFA labeling in human BLC-CO

WFA lectin-histochemistry in human subjects resulted in labeling of cells and perineuronal nets within specific BLC-CO subregions. Perineuronal nets showed evident hollow, mesh-like appearance and neuron-like shape (Fig 1A&B). Their morphological features suggests preferential association with large multipolar neurons, confirming previous reports in human and nonhuman primate amygdala (Hartig, et al., 1995,Pantazopoulos, et al., 2006). WFA intracellular labeling was not detected in cells with typical neuronal morphology. Cells with cytoplasmic WFA labeling consistently showed glial characteristics, for example small cell bodies and ‘bushy’, tightly packed, short processes (Fig 1B, C & E).

The specificity of WFA lectin histochemistry for CSPGs was tested by incubating sets of sections containing the amygdala from the same subjects in chondroitinase ABC, an enzyme known to degrade chondroitin sulfate glycosaminoglycan chains (Crespo, et al., 2007, Hamai, et al., 1997, Sugahara, et al., 1994). Chondroitinase ABC treatment resulted in complete disappearance of WFA-labeled glial cells; weakly stained perineuronal nets were occasionally detected in this material, possibly due to incomplete exposure to the enzyme.

Total numbers of WFA-labeled perineuronal nets

In the human BLC-CO, total numbers of perineuronal nets were estimated to be 515,008 ± 380,112 (mean ± standard deviation). The distribution of perineuronal nets in this nuclear complex, previously reported in human as well as monkey (Hartig, et al., 1995, Pantazopoulos, et al., 2006), shows preferential concentration in the LN (408,720 ± 300,669), followed by the BN (72,696 ± 72,239). Only few nets were detected in the ABN (18,096 ± 21,208) and CO (15,496 ± 8,348). As reported previously (Pantazopoulos, et al., 2006), and shown as an example in Fig. 2, perineuronal nets tend to cluster along the lateral portion of the LN, and in the magnocellular BN region.

Distribution, total numbers and numerical densities of WFA-labeled cells in the human amygdala

The total number of WFA-labeled glial cells in the human BLC-CO is estimated to be 175,568 ± 212,367 (mean ± standard deviation; Table 1). Of these, 102,232 ± 157,320 are in the LN, 52,832 ± 68,882 in the BN, 10,400 ± 15,872 in the ABN and 13,104 ± 11,656 in the CO.

Numerical densities of WFA-labeled cells are reported in Table 1. Linear regression models failed to detect any effect of age (R squared=0.05; p=0.41), cause of death (R squared=0.06; p=0.37), PMI (R squared=0.15; p=0.14), hemisphere (R squared=0.06; p=0.35), or gender (R squared=0.002; p=0.96) on total number of WFA-labeled cells in the LN, BN, ABN or CO. Numbers of WFA-labeled cells did not correlate significantly with numbers of perineuronal nets in any of the nuclei examined.

Although numbers of labeled cells vary substantially across subjects, their distribution within amygdalar nuclei is highly consistent. Approximately 57.2 % of these cells are found in the LN, particularly within its medial portion along its border with BN, and its ventrolateral portion concentrated primarily along its most ventral edge (Fig 3). The BN contains 29.6% of WFA-labeled cells, which are localized primarily within its parvicellular subregion. Typically, a group of these cells are found to mirror the cell cluster located along the ventro-medial edge of the medial LN. A smaller cell cluster is consistently detected in the magnocellular subregion of the BN. Only few WFA-labeled cells are located in the intermediate BN subnucleus. The ABN contains 5.8% of WFA-labeled cells, the majority of these are found in its dorsal portion. A cluster of these cells appears to extend into the central nucleus of the amygdala. The CO contains only approximately 7.3% of the WFA-labeled cells estimated over BLC-CO. These cells tend to cluster along its dorsal border, possibly extending into the medial and anterior amygdaloid nuclei (Fig 3). Although the distribution of labeled cells does not appear to vary substantially along the rostrocaudal axis of the BLC-CO, fewer cells were typically observed in the most caudal section used for the analysis.

Are WFA-labeled glial cells astrocytes?

The great majority of WFA-labeled glial cells in the human BLC-CO (93.7%) were also GFAP-immunoreactive. This percentage did not vary substantially across nuclei. In the LN, 92.9% of WFA-labeled glial cells were GFAP-positive, compared to 93.1% in the BN, 94.1% in the AB, and 94.6% in the CO. Cells showing immunoreactivity for GFAP but not WFA labeling were not counted in this study. These cells were overwhelmingly more numerous than WFA-labeled glial cells in all nuclei examined (Fig. 2).

WFA labeling in monkey and rat BLC-CO

In the amygdala of adult rhesus monkeys, WFA lectin-histochemistry labeled perineuronal nets were located primarily in the LN and BN, confirming results from a previous study by Hartig and collaborators (Hartig, et al., 1995) (Fig 4). Intracellular labeling was not observed in neurons or glial cells in any of the amygdala nuclei investigated. This finding was confirmed in all monkeys examined (n=6), ranging in age from 6 to 11 years old. Similarly, in the rat amygdala, WFA lectin-histochemistry labeled perineuronal nets located mainly in the BN and, to a lesser extent, LN (Fig 4). Again, intracellular labeling was not detected in the amygdala of rats aged 2, 4, and 8 months old.

To control for the possibility that tissue processing procedures may affect the capability to detect intracellular labeling in monkey and rat tissue, the brains from a separate group of rats (n=4) were processed using a protocol similar to that used for human tissue. Specifically, rats were sacrificed by pentobarbital overdose (130 mg/kg), their brains were removed fresh (no perfusion with fixative) and postfixed for 1 week before cryoprotection using the same solutions used for human tissue. Confirming our results, only perineuronal nets, but not intracellular glial or neuronal labeling, were detected in the amygdala of these rats. Thus, tissue processing is not likely to account for differences of WFA labeling in human as compared to rhesus monkey and rat.

4. DISCUSSION

The present results indicate that, in the BLC-CO of the normal human amygdala, CSPGs are expressed by a subpopulation of glial cells. A high percentage of these cells also expressed GFAP, indicating that they correspond to astrocytes. The distinct pattern of spatial distribution within each of the BLC-CO nuclei, consistently found in each subject, suggests that astrocytes expressing CSPGs may play a specific role in amygdalar functions. Intracellular labeling was not detected in neurons. As expected, perineuronal nets showed strong WFA labeling. In contrast to findings in human, WFA lectin histochemistry did not result in glial cell intracellular labeling in the amygdala of rhesus monkeys and rats. In these species, the spatial distribution pattern of labeled perineuronal nets was similar to that described in human and consistent with a previous report from Hartig et al (monkey) (Hartig, et al., 1995).

Technical Considerations

In the present study, WFA lectin histochemistry was used to detect CSPGs. The specificity of WFA as a marker for these macromolecules is supported by solid evidence from other groups as well as by the present results. WFA is known to bind to N-acetyl-galactosamine (Bruckner, et al., 1993, Celio, et al., 1998, Hartig, et al., 1994, Hartig, et al., 1992, Nakagawa, et al., 1986). This molecule is specifically represented, as a disaccharide unit bound to glucuronic acid, in the long chondroitin sulfate glycosaminoglycan chains characteristic of CSPGs (for review see Viapiano, et al., 2006). Furthermore, chondroitin sulfate glycosaminoglycans are not found in free form, but always attached to the core protein of the proteoglycans (Viapiano, et al., 2006), supporting the idea that WFA binding to N-acetyl-galactosamine allows detection of the entire CSPG molecule. A study reporting virtually identical patterns of perineuronal net labeling obtained with two different methods – WFA lectin-histochemistry and immunostaining using CSPG-specific antibodies – is consistent with this claim (Hartig, et al., 1994). It should also be noted that CSPGs, and lecticans in particular, are by far the most well represented proteoglycans in the brain extracellular matrix (Ruoslahti, 1996). Finally, in the present study, the specificity of WFA lectin histochemistry for CSPGs is demonstrated by control experiments with chondroitinase ABC, an enzyme that degrades chondroitin sulfate glycosaminoglycan chains and is routinely used to investigate the effects of elimination of CSPGs (e.g. Crespo, et al., 2007, Dityatev, et al., 2007, Hamai, et al., 1997, Pizzorusso, et al., 2002, Sugahara, et al., 1994). In our chondroitinase ABC-treated tissue, we could detect no intracellularly-labeled glia, and only rare, faintly labeled perineuronal nets.

GFAP is commonly used as an astrocytic marker (Eng, et al., 2000). This molecule constitutes the primary intermediate filament present in mature astrocytes of the central nervous system. Following injury, its synthesis and content within astrocytes increase rapidly resulting in a process termed reactive astrogliosis. However, under physiological conditions, GFAP is expressed by all mature astrocytes, where it provides structural stability to astrocytic processes and regulates motility (Eng, et al., 2000).

A caveat common to all immunocytochemical and histochemical methods is that some elements may express a specific marker at levels below those detectable with the available methods. In this study, it is possible that cells expressing low levels of CSPGs and/or GFAP may have gone undetected. On the one hand, failure to detect weakly labeled GFAP-immunoreactive cells may account for the small percentage (6–7%) of WFA-labeled cells not expressing GFAP. On the other hand, cells with CSPG expression below detection levels may or may not have also expressed GFAP. Although it is not possible at this stage to distinguish between these possibilities, the present results indicate that the great majority of cells expressing CSPGs in the normal adult amygdala are astrocytes.

Methods for data collection using light microscopy were based on modern stereology principles and adapted pragmatically to the requirements of histochemical procedures and distribution patterns of the objects to be counted (Benes, et al., 2001, Guillery, et al., 1997). Sections were selected using a systematic random sampling scheme and represented the whole rostrocaudal extent of the BLC-CO (Coggeshall, et al., 1996, Dorph-Petersen, et al., 2000, Gundersen, et al., 1999, West, 1999). Estimates of numerical densities obtained from these sections were confirmed using nuclei volume measurements in Nissl-stained serial sections (Berretta, et al., 2007). WFA-labeled cells and perineuronal nets were counted exhaustively within each amygdala nucleus in each section. Both cells and nets are sparsely represented and unevenly distributed. Exhaustive counts throughout each section allowed us to characterize their distribution and to increase the sensitivity in the X-Y plane, thus reducing the risk of underestimating poorly represented cell populations (Benes, et al., 2001). Furthermore, relatively thin sections (40 μm) were used in order to maximize the antibody penetration. These sections were found to collapse to a final estimated thickness of 5–6 μm. The ratio between the thickness of the optical dissector and that of neurons to be counted is not appropriate for the optical dissector method, while counts of nucleoli, or even nuclei, are not an viable option in WFA-stained sections. A recent study from our laboratory suggests modest heterogeneity of distribution of neurons across the depth of the section (Z axis) (Berretta, et al., 2007), possibly due to ‘lost caps’ factor (Gundersen, 1986, Hedreen, 1998) and/or uneven compression and/or shrinkage through the z-axis as a consequence of tissue processing (Gardella, et al., 2003). If such heterogeneity also affects perineuronal nets and glial cells in our tissue, counted exhaustively through the z-axis, the actual total cell numbers may be slightly higher than those reported here.

Distribution of WFA-labeling and functional implications

The expression of CSPGs has been shown to be dynamically regulated by a number of physiological stimuli during development as well as adult life (Dityatev, et al., 2007) (Galtrey, et al., 2007, Schwarzacher, et al., 2006, Smith, et al., 2005, Thon, et al., 2000, Yamaguchi, 2000). These macromolecules interact with growth factors, neurotransmitter receptors and voltage gated ion channels and may modulate plastic phenomena such as long term potentiation (Brakebusch, et al., 2002, Bukalo, et al., 2001, Dityatev, et al., 2003, Dityatev, et al., 2006, Viapiano, et al., 2006, Zhou, et al., 2001). Their synthesis is differentially regulated across developmental phases and is experience-dependent, as suggested by the observation that pericellular accumulations of secreted CSPGs, forming perineuronal nets, reach maturity in correspondence to the establishment of an adult pattern of synaptic connectivity (Dityatev, et al., 2007, Guimaraes, et al., 1990, Kalb, et al., 1990, Kalb, et al., 1990, Pizzorusso, et al., 2002). In adult, CSPGs expression was shown to be affected by neuronal activity and stimulation of GABA-A and glycine receptors (Dityatev, et al., 2007, Schwarzacher, et al., 2006). Such a broad range of functions and responsivity to physiological stimuli may account for the high degree of variability between subjects encountered in our study.

Overwhelming evidence also indicates that these molecules play important and diverse roles in the response to brain tissue damage, participating in axon growth inhibition and synaptic plasticity following lesions, as well as seizures (Beggah, et al., 2005, McKeon, et al., 1999, Naffah-Mazzacoratti, et al., 1999, Thon, et al., 2000, for review see Viapiano, et al., 2006). These considerations raise the question of whether, in our samples, CSPG expression in astrocytes may be attributable to physiological processes or, instead, reflect a pathological state, perhaps related to the relatively old age of the subjects included in this study. Several considerations point to the former, suggesting a functional role of CSPGs in the normal amygdala. First, total numbers, as well as numerical densities, of WFA-labeled glial cells did not correlate with age or cause of death. Although, expression of CSPGs in glial cells may vary through adulthood, these results suggest that ageing processes and/or prolonged agonal states,

are not likely to induce substantial increases of CSPG-expressing astrocytes. Second, WFA-labeled glial cells were detected in the youngest human subject in our cohort (37 years old), but not in the oldest monkeys in our study, whose age (11 years old, n=2; 10.9 years old, n=1), approximates mid-thirties of human age. Third, the between subjects consistency of the distribution of WFA-labeled glial cells in human, characterized by small clusters consistently segregated within specific portions of the BLC-CO, suggests an association with specific physiological properties of these subregions, rather than with a range of brain insults.

To this effect, the relative spatial distribution of neurons expressing parvalbumin, perineuronal nets and CSPG-expressing astrocytes in the amygdala may provide some clues. Approximately 68% of perineuronal nets in the basolateral complex of the amygdala is associated with neurons expressing parvalbumin; not surprisingly the distribution of these two elements overlaps largely, with the highest concentration in the lateral nucleus (Fig. 2) (see also Pantazopoulos, et al., 2006). It is possible that the spatial segregation of CSPG-expressing astrocytes in the amygdala may be, at least in part, related to the distribution of amygdala neurons expressing parvalbumin and associated with perineuronal nets. In fact, the prevalence and distribution of these neurons, as well as that of WFA-labeled perineuronal nets, in each of the nuclei investigated are similar to that of CSPG-expressing (WFA-GFAP-positive) astrocytes (Fig. 2). However, a functional relationship between these elements may be just one of several functions of these cells, as suggested by lack of significant correlations between numbers of perineuronal nets and WFA-labeled astrocytes as well as findings showing that levels of CSPGs expression in astrocytes are modulated by neuronal activity (Schwarzacher, et al., 2006). Speculatively, the distribution of these cells within the amygdala may also be related to termination fields of particularly active extrinsic inputs.

Another possible clue points to the role of CSPGs during development, when these molecules form inhibitory barriers guiding neuronal migration and axonal growth (e.g. Carulli, et al., 2005, Masuda, et al., 2005, Viapiano, et al., 2006). The anatomical distribution pattern of WFA-labeled astrocytes characterized in our study is highly reminiscent of cellular migratory routes in the amygdala. For instance, the majority of WFA-labeled astrocytes within the BLC-CO are distributed along its ventral portion. During the fifth gestational month, cell-dense columns, considered migratory streams, emerge from the human ganglionic eminence, located ventrally with respect to the amydgala, and reach into the basolateral complex (LN, BN and ABN) (Nikolic, et al., 1986, Ulfig, et al., 2003). During the following months, these migratory streams lose their connection with the proliferative zone and can no longer be detected at nine months (Ulfig, et al., 1998, Ulfig, et al., 2003). On a speculative level, it is tempting to suggest that CSPG-expressing glial cells concentrated along the ventral portion of LN and BN may play a role in guiding neuronal migratory streams arising from the ganglionic eminence and/or providing a barrier for further migration during late gestational months.

Selective expression of CSPGs in astrocytes in the normal human amygdala

Studies in rodent and cell cultures have shown that distinct members of the CSPG family are synthesized and expressed by several different cell types (for review see Carulli, et al., 2006, Viapiano, et al., 2006). Brevican, and to a lesser extent neurocan, are commonly associated with astrocytes (Carulli, et al., 2006, McKeon, et al., 1999, Thon, et al., 2000, Viapiano, et al., 2006). In contrast, versican is commonly expressed in oligodendrocytes and NG2-positive oligodendrocyte precursors, and aggrecan is mainly detected in neurons (Carulli, et al., 2006, Viapiano, et al., 2006). The present results are in contrast with this evidence, as they suggest that in the human amygdala, but not in rat or monkey (Fig 4), astrocytes may be the main source of CSPGs. Although, at least in principle, this is possible, other interpretations must be considered. As mentioned above, other cells, such as neurons and oligodendrocytes, may express CSPGs at low, but still functionally relevant, levels that may fall below the detection

levels of our method. Alternatively, brevican may be the CSPGs primarily expressed in the adult normal human amygdala. Differential selectivity of WFA cytochemistry for human CSPGs expressed in astrocytes is not likely since WFA binds to one of the most basic shared components of these molecules (Bruckner, et al., 1993, Celio, et al., 1998, Hartig, et al., 1994, Hartig, et al., 1992, Nakagawa, et al., 1986).

5. Conclusions

The present results show that, in the adult human amygdala, CSPGs are mainly expressed by a subpopulation of astrocytes. Although these results do not rule out the possibility that neurons, oligodendrocytes and oligodendrocyte precursor cells may express low levels of CSPGs, they show that, in human, astrocytes express by far the highest levels of these molecules. The remarkable distribution pattern of CSPG-expressing astrocytes within the BLC-CO points to a distinct physiological role of CSPGs within specific amygdala subregions. Intriguingly, no CSPG expression was detected in rat and nonhuman primate glial cells, suggesting species specificity.

EXPERIMENTAL PROCEDURES

Human Subjects and Tissue Processing

Brain tissue blocks containing the whole amygdala from adult normal human donors (n=15), were obtained from the Harvard Brain Tissue Resource Center (HBTRC) (Table 2). Blocks were dissected fresh from whole brains upon arrival at the HBTRC and immediately placed in 4% paraformaldehyde. The blocks were stored in 0.1 M phosphate buffer (PB) containing 4% paraformaldehyde for two weeks followed by one week in cryoprotectant solution (30% glycerol, 30% ethylene glycol, 0.1% NaAzide in PB). Blocks were then cut into sequential 2 mm coronal slabs using an antithetic tissue slicer and resectioned into 40μm serial sections on a freezing microtome (American Optical 860, Buffalo, NY). This method is well suited for measurements of volume and total cell numbers because it allows optimal tissue preservation, and avoids distortion and excessive variations of section thickness and tissue loss due to temperature changes that often occur while slicing a large cryoprotected tissue block. Incomplete sectioning due to alignment of the slab on the microtome amounted to a thickness of no more than 80–100 μm/slab. Sections were stored in the same cryoprotectant solution at −20 °C. Tissue from several regions from each brain was analyzed by a neuropathologist to determine any evidence of gross and/or macroscopic changes consistent with Alzheimer's disease and other neurological illnesses, cerebrovascular accident, ethanol abuse, or other confounding factors.

Nonhuman Primate Subjects and Tissue Processing

Monkeys were given a lethal dose of sodium pentobarbital (100 mg/kg, i.p.) and were perfused intracardially with normal saline followed by a solution of 4% paraformaldehyde in 0.1 M phosphate buffer. The brains were removed, photographed, and placed in solutions of 10% (for 1 day) followed by 20% (for 4–5 days) glycerol plus 2% DMSO in 0.1 M phosphate buffer for cryoprotection. Then the brain was frozen in isopentane overnight and cut on a freezing microtome at 40 μm in the coronal plane. All sections were collected and saved in a solution for long-term storage consisting of 30% glycerol and 30% ethylene glycol in 0.1 M phosphate buffer.

Rat Tissue Processing

Male Sprague-Dawley rats (n=30 total; P240 n= 2; P120, n=5; P60, n=6; P45, n=5, P30, n=6, P15, n=6; Charles River Laboratories Inc., Wilmington, MA) were sacrificed by an overdose of sodium pentobarbital (130 mg/kg) and perfused with fixative (200 ml, 4% paraformaldheyde

in 0.1 M PB). Brains were collected, postfixed (1 hr), cryoprotected (20% glycerol in 0.1 M PB overnight). A separate group of four rats (P60) was sacrificed by an overdose of sodium pentobarbital (130 mg/kg) but not perfused with fixative; after removal, the brains were postfixed for 1 week in 4% paraformaldehyde, then placed in cryoprotectant solution (30% glycerol, 30% ethylene glycol, 0.1% NaAzide in PB) until it sank to the bottom of the jar. Sections from all rat brains were serially sliced (30 μm) in coronal sections on a freezing microtome (American Optical 860, Buffalo, NY). Sets of serial sections including the whole rotrocaudal extent of the amygdala were used for histochemitry.

Histochemistry

For human and monkey tissue, free-floating sections were incubated in citric acid buffer (0.1 M citric acid, 0.2 M Na_2HPO_4) heated to 80 °C for 30 minutes, then incubated in biotinylated WFA (1:500 μl; Vector Labs, Burlingame, CA) in 1% bovine albumine serum (BSA) for 24 hr at 4 °C. Sections were then incubated in streptavidin conjugated with horse radish peroxidase (1:5000 μl, Zymed, San Francisco, CA), and, finally, in nickel-enhanced diaminobenzidine/peroxidase reaction (0.02% diaminobenzidine, Sigma-Aldrich, 0.08% nickel-sulphate, 0.006% hydrogen peroxide) for visualization of the reaction product. Solutions for all the following steps were made in PBS with 0.5% Triton X (PBS-Tx). Each step was followed by washes in the same solution. Sections were counterstained with methyl green nuclear stain (Vector Labs, Burlingame, CA) and coverslipped. WFA histochemistry for rat tissue was identical to the one described above, with the exception that no antigen unmasking procedure was performed and buffers contained 0.2 % Tx.

For chondroitinase ABC digestion, following antigen unmasking with citric acid buffer, human amygdala sections were incubated overnight at 37 degrees °C in chondroitinase buffer consisting of 250 μl of chondroitinase ABC (10mU/μl, cat #C-2905, Sigma-Aldrich, St. Louis, MO) in 2ml of chondroitinase buffer (50 mM Tris, pH 8.0, 60 mM sodium acetate, and 0.02% BSA).

Dual Fluorescent Immunocytochemistry

A subset of five amygdalas from five different donors was used for dual fluorescent labeling. Free-floating sections were processed for antigen unmasking as above and then incubated in 5% BSA (1 hr) and placed in monoclonal primary antisera raised in mouse against glial fibrillary acidic protein (GFAP) (1:8,000 μl, G 3893, Sigma-Aldrich, St. Louis, MO) in 1% BSA at 4 degrees C for 72 hr. Immunoblotting assays show that this antibody is highly specific for GFAP and does not cross react with vimentin. Astrocytes, Bergmann glial cells, gliomas, and other glial cell derived tumors are specifically detected using this antibody (information provided by Sigma-Aldrich, St. Louis, MO). Sections were then incubated for 4 hr with Alexa Fluor horse anti-mouse (1:250 μl; wave length: 555) for 4 hr. Following several rinses, sections were placed in a solution containing biotinylated WFA (1:500 μl, Vector Labs, Burlingame, CA) in 1% BSA for 24 hr at 4 °C, followed by 4 hr incubation in Alexa Fluor Streptavidin (wave length: 488; 1:2000 μl). Solutions for all the steps above were made in PBS with 0.5% Triton X (PBS-Tx). Each step was followed by washes in the same solution. To eliminate lipofuscin autofluorescence, sections were incubated in 1mM CuSO4 for 10 minutes (Schnell, et al., 1999). Sections were coverslipped with anti-fade Gel/Mount (Biomeda Corp., Foster City, CA). All fluorescent probes were purchased from Molecular Probes Inc. Eugene, OR.

Data Collection for Human Tissue

Light Microscopy—Four serial representative sections from each amygdala (section interval, 1040 μm), were labeled with WFA lectin histochemistry, counterstained with methyl green nuclear staining, and matched across subjects for rostral-caudal level according to morphological and cytoarchitectonic criteria as described previously (Pantazopoulos, et al.,

2006) (Fig. 3). A Zeiss Axioskop 2 Plus interfaced with StereoInvestigator 6.0 (Microbrightfield Inc., Willinston, VT) was used for analysis. The borders of each of the nuclei examined in this study, i.e. LN, BN, AB and CO, were delineated with a 1.6x objective according to well-established cytoarchitectonic criteria (Amaral, et al., 1992, Gloor, 1997, Sorvari, et al., 1995). Sections were then scanned through the extent of the x, y, and z-axes using a 40x objective. On the basis of a previous knowledge (Bruckner, et al., 1994, Hamidi, et al., 2004, Pantazopoulos, et al., 2006), the following criteria were established for classification of WFA-labeled objects. WFA-labeled glial cells are characterized by clearly distinguishable intracellular labeling and a small, round body surrounded by a multitude of short, thin and tightly packed (bush-like) processes (Fig 1B,& E). WFA-labeled neurons show intracellular labeling and clear neuronal morphology (Luth, et al., 1992). Perineuronal nets are typically distinguished easily from labeled cells, as they show neuron-like morphology, i.e. relatively large, polygonal or fusiform cell bodies and a small number of distinct primary dendrites, but the labeling has a hollow appearance, with a mesh-like, pericellular pattern (Fig. 1D&F).

Fluorescent Microscopy—Quantitative analysis of double-labeled cells was performed using a Zeiss Axioscope 2 plus system equipped with FITC and TRITC filters and interfaced with Stereo-Investigator 6.0 image analysis software. Sections used for light microscopy WFA detection were adjacent to dual fluorescence labeled sections, and were used for tracing the borders of the LN, BN, ABN and CO on the latter (Amaral, et al., 1992, Gloor, 1997, Sorvari, et al., 1995). Each nucleus was scanned systematically in its whole dorso-ventral and latero-medial extent and throughout the z-axis, using a 40x objective and fluorescent filters TRITC, 555 (GFAP) and FITC 488 (WFA). All WFA-labeled cells were recorded according to presence of WFA labeling alone or together with GFAP expression (Fig. 1). Co-localization was determined by overlaying the image captured using the TRITC filter and the FITC filter using Stereo-Investigator software.

Confocal Microscopy—Confocal microscopy was used to confirm data obtained with fluorescent microscopy. Approximately 20% of the WFA-labeled cells were re-sampled using a Leica Confocal Microscope System equipped with TRITC and FITC filters. This system allows scanning through the z-axis of each section in 1 μm increments, thus resolving among two or more neurons sharing the same Y and X (but not Z) coordinates. Co-localization of two markers was established when the respective fluorescence signal was clearly present at the same range within the z-axis for each marker examined and confirmed by a color change of overlapping markers (Fig 1F). Results obtained with confocal and fluorescence microscopy were virtually identical, confirming the validity of the latter.

Statistical Analysis

Total number (Tn) of WFA-labeled, putatively CSPGs-positive, cells was calculated as $\boldsymbol{Tn = i \bullet \Sigma n}$, where $\boldsymbol{\Sigma n}$ = sum of the cells counted in each subject, and $\boldsymbol{i}$ is the section interval (i.e. number of serial sections between each section and the next within each compartment, i.e. 26) as described in detail in previous work (Pantazopoulos, et al., 2006). Stepwise linear regression models were used to analyze the effects of age, postmortem time interval (PMI), cause of death (acute vs chronic), hemisphere, and gender on total numbers of WFA-labeled cells and of percentages of WFA-labeled cells showing GFAP immunoreactivity using JMP v5.0.1a (SAS Institute Inc., Cary, NC). Microphotographs and figures were processed using Adobe Illustrator CS (Adobe Systems Inc., San Jose, CA). No adjustments were made to any aspect of the original photos except for size reduction.

Data Collection for Monkey and Rat Tissue

Sections from rhesus monkey and rat, containing the amygdala and stained with WFA lectin histochemistry were examined under light microscopy. Each amygdala nucleus was scanned systematically in its rostro-caudal, latero-medial and dorso-ventral extent. Each labeled element was examined and recorded according to morphological criteria and presence of intracellular labeling according to the same criteria described for human tissue.

Acknowledgments

Funding Support: This work was supported by NIH grants MH063215 and MH066280 to SB and the Andrew P Merrill Foundation to HP.

The authors thank the Harvard Brain Tissue Resource Center, funded by NIH R24MH068855 and directed by Dr. F. M. Benes, for providing the tissue used in these investigations.

LIST OF ABREVIATIONS

ABN
accessory basal nucleus

BLC-CO
lateral, basal, accessory basal, and cortical nuclei of the amygdala

BN
basal nucleus

BSA
bovine albumine serum

CO
cortical nucleus

CSPGs
chondroitin sulphate proteoglycans

ECM
extracellular matrix

GFAP
glial fibrillary acidic protein

LN
lateral nucleus

Nd
numerical density

Tn
total number

PMI
post-mortem interval

WFA
wisteria floribunda agglutinin

References

Akbarian S, Kim JJ, Potkin SG, Hetrick WP, Bunney WE Jr, Jones EG. Maldistribution of interstitial neurons in prefrontal white matter of the brains of schizophrenic patients. Arch Gen Psychiatry 1996;53:425–436. [PubMed: 8624186]

Amaral, DG.; Price, JL.; Pitkanen, A.; Carmichael, ST. Anatomical organization of the primate amygdaloid complex. J.P. Aggleton, Wiley-Liss; New York: 1992.

Arnold SE, Hyman BT, Van Hoesen GW, Damasio AR. Some cytoarchitectural abnormalities of the entorhinal cortex in schizophrenia. Arch Gen Psychiatry 1991;48:625–632. [PubMed: 2069493]

Bandtlow CE, Zimmermann DR. Proteoglycans in the developing brain: new conceptual insights for old proteins. Physiol Rev 2000;80:1267–1290. [PubMed: 11015614]

Beggah AT, Dours-Zimmermann MT, Barras FM, Brosius A, Zimmermann DR, Zurn AD. Lesion-induced differential expression and cell association of Neurocan, Brevican, Versican V1 and V2 in the mouse dorsal root entry zone. Neuroscience 2005;133:749–762. [PubMed: 15896911]

Benes FM, Lange N. Two-dimensional versus three-dimensional cell counting: a practical perspective. Trends Neurosci 2001;24:11–17. [PubMed: 11163882]

Berghuis P, Dobszay MB, Sousa KM, Schulte G, Mager PP, Hartig W, Gorcs TJ, Zilberter Y, Ernfors P, Harkany T. Brain-derived neurotrophic factor controls functional differentiation and microcircuit formation of selectively isolated fast-spiking GABAergic interneurons. Eur J Neurosci 2004;20:1290–1306. [PubMed: 15341601]

Berretta S, Pantazopoulos H, Lange N. Neuron numbers and volume of the amygdala in subjects diagnosed with bipolar disorder or schizophrenia. Biol Psychiatry 2007;62:884–893. [PubMed: 17698040]

Bovolenta P, Fernaud-Espinosa I. Nervous system proteoglycans as modulators of neurite outgrowth. Prog Neurobiol 2000;61:113–132. [PubMed: 10704995]

Brakebusch C, Seidenbecher CI, Asztely F, Rauch U, Matthies H, Meyer H, Krug M, Bockers TM, Zhou X, Kreutz MR, Montag D, Gundelfinger ED, Fassler R. Brevican-deficient mice display impaired hippocampal CA1 long-term potentiation but show no obvious deficits in learning and memory. Mol Cell Biol 2002;22:7417–7427. [PubMed: 12370289]

Bruckner G, Brauer K, Hartig W, Wolff JR, Rickmann MJ, Derouiche A, Delpech B, Girard N, Oertel WH, Reichenbach A. Perineuronal nets provide a polyanionic, glia-associated form of microenvironment around certain neurons in many parts of the rat brain. Glia 1993;8:183–200. [PubMed: 7693589]

Bruckner G, Seeger G, Brauer K, Hartig W, Kacza J, Bigl V. Cortical areas are revealed by distribution patterns of proteoglycan components and parvalbumin in the Mongolian gerbil and rat. Brain Res 1994;658:67–86. [PubMed: 7834357]

Bruckner G, Szeoke S, Pavlica S, Grosche J, Kacza J. Axon initial segment ensheathed by extracellular matrix in perineuronal nets. Neuroscience 2006;138:365–375. [PubMed: 16427210]

Bukalo O, Schachner M, Dityatev A. Modification of extracellular matrix by enzymatic removal of chondroitin sulfate and by lack of tenascin-R differentially affects several forms of synaptic plasticity in the hippocampus. Neuroscience 2001;104:359–369. [PubMed: 11377840]

Carulli D, Laabs T, Geller HM, Fawcett JW. Chondroitin sulfate proteoglycans in neural development and regeneration. Curr Opin Neurobiol 2005;15:116–120. [PubMed: 15721753]

Carulli D, Rhodes KE, Brown DJ, Bonnert TP, Pollack SJ, Oliver K, Strata P, Fawcett JW. Composition of perineuronal nets in the adult rat cerebellum and the cellular origin of their components. J Comp Neurol 2006;494:559–577. [PubMed: 16374793]

Celio MR, Spreafico R, De Biasi S, Vitellaro-Zuccarello L. Perineuronal nets: past and present. Trends Neurosci 1998;21:510–515. [PubMed: 9881847]

Coggeshall RE, Lekan HA. Methods for determining number of cells and synapses: a case for more uniform standard of review. J Comp Neurol 1996;364:6–15. [PubMed: 8789272]

Corfas G, Roy K, Buxbaum JD. Neuregulin 1-erbB signaling and the molecular/cellular basis of schizophrenia. Nat Neurosci 2004;7:575–580. [PubMed: 15162166]

Corvetti L, Rossi F. Degradation of chondroitin sulfate proteoglycans induces sprouting of intact Purkinje axons in the cerebellum of the adult rat. J Neurosci 2005;25:7150–7158. [PubMed: 16079397]

Costa E, Davis JM, Dong E, Grayson DR, Guidotti A, Tremolizzo L, Veldic M. A GABAergic cortical deficit dominates schizophrenia pathophysiology. Crit Rev Neurobiol 2004;16:1–23. [PubMed: 15581395]

Crespo D, Asher RA, Lin R, Rhodes KE, Fawcett JW. How does chondroitinase promote functional recovery in the damaged CNS? Exp Neurol 2007;206:159–171. [PubMed: 17572406]

Deepa SS, Carulli D, Galtrey C, Rhodes K, Fukuda J, Mikami T, Sugahara K, Fawcett JW. Composition of perineuronal net extracellular matrix in rat brain: a different disaccharide composition for the net-associated proteoglycans. J Biol Chem 2006;281:17789–17800. [PubMed: 16644727]

Dityatev A, Bruckner G, Dityateva G, Grosche J, Kleene R, Schachner M. Activity-dependent formation and functions of chondroitin sulfate-rich extracellular matrix of perineuronal nets. Dev Neurobiol 2007;67:570–588. [PubMed: 17443809]

Dityatev A, Schachner M. Extracellular matrix molecules and synaptic plasticity. Nat Rev Neurosci 2003;4:456–468. [PubMed: 12778118]

Dityatev A, Schachner M. The extracellular matrix and synapses. Cell Tissue Res. 2006

Dong E, Agis-Balboa RC, Simonini MV, Grayson DR, Costa E, Guidotti A. Reelin and glutamic acid decarboxylase67 promoter remodeling in an epigenetic methionine-induced mouse model of schizophrenia. Proc Natl Acad Sci U S A 2005;102:12578–12583. [PubMed: 16113080]

Dorph-Petersen KA, Gundersen HJ, Jensen EB. Non-uniform systematic sampling in stereology. J Microsc 2000;200(Pt 2):148–157. [PubMed: 11106955]

Eastwood SL, Law AJ, Everall IP, Harrison PJ. The axonal chemorepellant semaphorin 3A is increased in the cerebellum in schizophrenia and may contribute to its synaptic pathology. Mol Psychiatry 2003;8:148–155. [PubMed: 12610647]

Eng LF, Ghirnikar RS, Lee YL. Glial fibrillary acidic protein: GFAP-thirty-one years (1969–2000). Neurochemical Research 2000;25:1439–1451. [PubMed: 11059815]

Falkai P, Schneider-Axmann T, Honer WG. Entorhinal cortex pre-alpha cell clusters in schizophrenia: quantitative evidence of a developmental abnormality. Biol Psychiatry 2000;47:937–943. [PubMed: 10838061]

Galtrey CM, Fawcett JW. The role of chondroitin sulfate proteoglycans in regeneration and plasticity in the central nervous system. Brain Res Rev 2007;54:1–18. [PubMed: 17222456]

Gardella D, Hatton WJ, Rind HB, Rosen GD, von Bartheld CS. Differential tissue shrinkage and compression in the z-axis: implications for optical disector counting in vibratome-, plastic- and cryosections. J Neurosci Methods 2003;124:45–59. [PubMed: 12648764]

Gloor, P. The temporal lobe and limbic system. Oxford University Press; New York: 1997. The amygdaloid system; p. 591-721.

Guidotti A, Auta J, Davis JM, Di-Giorgi-Gerevini V, Dwivedi Y, Grayson DR, Impagnatiello F, Pandey G, Pesold C, Sharma R, Uzunov D, Costa E. Decrease in reelin and glutamic acid decarboxylase67 (GAD67) expression in schizophrenia and bipolar disorder: a postmortem brain study. Arch Gen Psychiatry 2000;57:1061–1069. [PubMed: 11074872]

Guidotti A, Pesold C, Costa E. New neurochemical markers for psychosis: a working hypothesis of their operation. Neurochem Res 2000;25:1207–1218. [PubMed: 11059795]

Guillery RW, Herrup K. Quantification without pontification: choosing a method for counting objects in sectioned tissues. J Comp Neurol 1997;386:2–7. [PubMed: 9303520]

Guimaraes A, Zaremba S, Hockfield S. Molecular and morphological changes in the cat lateral geniculate nucleus and visual cortex induced by visual deprivation are revealed by monoclonal antibodies Cat-304 and Cat-301. J Neurosci 1990;10:3014–3024. [PubMed: 1697900]

Gundersen HJ. Stereology of arbitrary particles. A review of unbiased number and size estimators and the presentation of some new ones, in memory of William R. Thompson. J Microsc 1986;143(Pt 1): 3–45. [PubMed: 3761363]

Gundersen HJ, Jensen EB, Kieu K, Nielsen J. The efficiency of systematic sampling in stereology--reconsidered. J Microsc 1999;193:199–211. [PubMed: 10348656]

Hahn CG, Wang HY, Cho DS, Talbot K, Gur RE, Berrettini WH, Bakshi K, Kamins J, Borgmann-Winter KE, Siegel SJ, Gallop RJ, Arnold SE. Altered neuregulin 1-erbB4 signaling contributes to NMDA receptor hypofunction in schizophrenia. Nat Med 2006;12:824–828. [PubMed: 16767099]

Hamai A, Hashimoto N, Mochizuki H, Kato F, Makiguchi Y, Horie K, Suzuki S. Two distinct chondroitin sulfate ABC lyases. An endoeliminase yielding tetrasaccharides and an exoeliminase preferentially acting on oligosaccharides. J Biol Chem 1997;272:9123–9130. [PubMed: 9083041]

Hamel MG, Mayer J, Gottschall PE. Altered production and proteolytic processing of brevican by transforming growth factor beta in cultured astrocytes. J Neurochem 2005;93:1533–1541. [PubMed: 15935069]

Hamidi M, Drevets WC, Price JL. Glial reduction in amygdala in major depressive disorder is due to oligodendrocytes. Biological Psychiatry 2004;55:563–569. [PubMed: 15013824]

Harrison PJ, Law AJ. Neuregulin 1 and schizophrenia: genetics, gene expression, and neurobiology. Biol Psychiatry 2006;60:132–140. [PubMed: 16442083]

Hartig W, Brauer K, Bigl V, Bruckner G. Chondroitin sulfate proteoglycan-immunoreactivity of lectin-labeled perineuronal nets around parvalbumin-containing neurons. Brain Res 1994;635:307–311. [PubMed: 8173967]

Hartig W, Brauer K, Bruckner G. Wisteria floribunda agglutinin-labelled nets surround parvalbumin-containing neurons. Neuroreport 1992;3:869–872. [PubMed: 1421090]

Hartig W, Bruckner G, Brauer K, Schmidt C, Bigl V. Allocation of perineuronal nets and parvalbumin-, calbindin- D28k- and glutamic acid decarboxylase-immunoreactivity in the amygdala of the rhesus monkey. Brain Res 1995;698:265–269. [PubMed: 8581495]

Hartmann U, Maurer P. Proteoglycans in the nervous system--the quest for functional roles in vivo. Matrix Biol 2001;20:23–35. [PubMed: 11246001]

Hedreen JC. Lost caps in histological counting methods. Anat Rec 1998;250:366–372. [PubMed: 9517853]

Jakob H, Beckmann H. Prenatal developmental disturbances in the limbic allocortex in schizophrenics. J Neural Transm 1986;65:303–326. [PubMed: 3711886]

Jakob H, Beckmann H. Circumscribed malformation and nerve cell alterations in the entorhinal cortex of schizophrenics. Pathogenetic and clinical aspects. J Neural Transm Gen Sect 1994;98:83–106. [PubMed: 7734114]

John N, Krugel H, Frischknecht R, Smalla KH, Schultz C, Kreutz MR, Gundelfinger ED, Seidenbecher CI. Brevican-containing perineuronal nets of extracellular matrix in dissociated hippocampal primary cultures. Mol Cell Neurosci 2006;31:774–784. [PubMed: 16503162]

Kalb RG, Hockfield S. Induction of a neuronal proteoglycan by the NMDA receptor in the developing spinal cord. Science 1990;250:294–296. [PubMed: 2145629]

Kalb RG, Hockfield S. Large diameter primary afferent input is required for expression of the Cat-301 proteoglycan on the surface of motor neurons. Neuroscience 1990;34:391–401. [PubMed: 2333149]

Kinsella MG, Bressler SL, Wight TN. The regulated synthesis of versican, decorin, and biglycan: extracellular matrix proteoglycans that influence cellular phenotype. Crit Rev Eukaryot Gene Expr 2004;14:203–234. [PubMed: 15248816]

Kovalenko S, Bergmann A, Schneider-Axmann T, Ovary I, Majtenyi K, Havas L, Honer WG, Bogerts B, Falkai P. Regio entorhinalis in schizophrenia: more evidence for migrational disturbances and suggestions for a new biological hypothesis. Pharmacopsychiatry 2003;36(Suppl 3):S158–161. [PubMed: 14677073]

Longson D, Deakin JF, Benes FM. Increased density of entorhinal glutamate-immunoreactive vertical fibers in schizophrenia. J Neural Transm 1996;103:503–507. [PubMed: 9617791]

Luth HJ, Fischer J, Celio MR. Soybean lectin binding neurons in the visual cortex of the rat contain parvalbumin and are covered by glial nets. J Neurocytol 1992;21:211–221. [PubMed: 1560253]

Masuda T, Shiga T. Chemorepulsion and cell adhesion molecules in patterning initial trajectories of sensory axons. Neurosci Res 2005;51:337–347. [PubMed: 15740797]

McKeon RJ, Jurynec MJ, Buck CR. The chondroitin sulfate proteoglycans neurocan and phosphacan are expressed by reactive astrocytes in the chronic CNS glial scar. J Neurosci 1999;19:10778–10788. [PubMed: 10594061]

McKeon RJ, Schreiber RC, Rudge JS, Silver J. Reduction of neurite outgrowth in a model of glial scarring following CNS injury is correlated with the expression of inhibitory molecules on reactive astrocytes. J Neurosci 1991;11:3398–3411. [PubMed: 1719160]

Morgenstern DA, Asher RA, Fawcett JW. Chondroitin sulphate proteoglycans in the CNS injury response. Prog Brain Res 2002;137:313–332. [PubMed: 12440375]

Morris NP, Henderson Z. Perineuronal nets ensheath fast spiking, parvalbumin-immunoreactive neurons in the medial septum/diagonal band complex. Eur J Neurosci 2000;12:828–838. [PubMed: 10762312]

Naffah-Mazzacoratti MG, Arganaraz GA, Porcionatto MA, Scorza FA, Amado D, Silva R, Bellissimo MI, Nader HB, Cavalheiro EA. Selective alterations of glycosaminoglycans synthesis and proteoglycan expression in rat cortex and hippocampus in pilocarpine-induced epilepsy. Brain Res Bull 1999;50:229–239. [PubMed: 10582521]

Nakagawa F, Schulte BA, Spicer SS. Selective cytochemical demonstration of glycoconjugate-containing terminal N-acetylgalactosamine on some brain neurons. J Comp Neurol 1986;243:280–290. [PubMed: 3944281]

Nikolic I, Kostovic I. Development of the lateral amygdaloid nucleus in the human fetus: transient presence of discrete cytoarchitectonic units. Anat Embryol (Berl) 1986;174:355–360. [PubMed: 3766991]

Okamoto M, Mori S, Endo H. A protective action of chondroitin sulfate proteoglycans against neuronal cell death induced by glutamate. Brain Res 1994;637:57–67. [PubMed: 7910106]

Pantazopolous, H.; Berretta, S. Glial Cells Abnormalities in the Amygdala and Entorhinal Cortex of Subjects with Schizophrenia. Society for Neuroscience; Atlanta, GA: 2006.

Pantazopoulos H, Lange N, Hassinger L, Berretta S. Subpopulations of neurons expressing parvalbumin in the human amygdala. J Comp Neurol 2006;496:706–722. [PubMed: 16615121]

Perosa SR, Porcionatto MA, Cukiert A, Martins JR, Passeroti CC, Amado D, Matas SL, Nader HB, Cavalheiro EA, Leite JP, Naffah-Mazzacoratti MG. Glycosaminoglycan levels and proteoglycan expression are altered in the hippocampus of patients with mesial temporal lobe epilepsy. Brain Res Bull 2002;58:509–516. [PubMed: 12242104]

Pizzorusso T, Medini P, Berardi N, Chierzi S, Fawcett JW, Maffei L. Reactivation of ocular dominance plasticity in the adult visual cortex. Science 2002;298:1248–1251. [PubMed: 12424383]

Rauch U, Feng K, Zhou XH. Neurocan: a brain chondroitin sulfate proteoglycan. Cell Mol Life Sci 2001;58:1842–1856. [PubMed: 11766883]

Rhodes KE, Fawcett JW. Chondroitin sulphate proteoglycans: preventing plasticity or protecting the CNS? J Anat 2004;204:33–48. [PubMed: 14690476]

Ruoslahti E. Brain extracellular matrix. Glycobiology 1996;6:489–492. [PubMed: 8877368]

Schnell SA, Staines WA, Wessendorf MW. Reduction of lipofuscin-like autofluorescence in fluorescently labeled tissue. J Histochem Cytochem 1999;47:719–730. [PubMed: 10330448]

Schwarzacher SW, Vuksic M, Haas CA, Burbach GJ, Sloviter RS, Deller T. Neuronal hyperactivity induces astrocytic expression of neurocan in the adult rat hippocampus. Glia 2006;53:704–714. [PubMed: 16498620]

Smith GM, Strunz C. Growth factor and cytokine regulation of chondroitin sulfate proteoglycans by astrocytes. Glia 2005;52:209–218. [PubMed: 15968632]

Sobel RA, Ahmed AS. White matter extracellular matrix chondroitin sulfate/dermatan sulfate proteoglycans in multiple sclerosis. J Neuropathol Exp Neurol 2001;60:1198–1207. [PubMed: 11764092]

Sorvari H, Soininen H, Paljarvi L, Karkola K, Pitkanen A. Distribution of parvalbumin-immunoreactive cells and fibers in the human amygdaloid complex. J Comp Neurol 1995;360:185–212. [PubMed: 8522643]

Sugahara K, Shigeno K, Masuda M, Fujii N, Kurosaka A, Takeda K. Structural studies on the chondroitinase ABC-resistant sulfated tetrasaccharides isolated from various chondroitin sulfate isomers. Carbohydr Res 1994;255:145–163. [PubMed: 8181004]

Thon N, Haas CA, Rauch U, Merten T, Fassler R, Frotscher M, Deller T. The chondroitin sulphate proteoglycan brevican is upregulated by astrocytes after entorhinal cortex lesions in adult rats. Eur J Neurosci 2000;12:2547–2558. [PubMed: 10947829]

Ulfig N, Setzer M, Bohl J. Transient architectonic features in the basolateral amygdala of the human fetal brain. Acta Anat (Basel) 1998;163:99–112. [PubMed: 9873139]

Ulfig N, Setzer M, Bohl J. Ontogeny of the human amygdala. Ann N Y Acad Sci 2003;985:22–33. [PubMed: 12724145]

Vawter MP, Frye MA, Hemperly JJ, VanderPutten DM, Usen N, Doherty P, Saffell JL, Issa F, Post RM, Wyatt RJ, Freed WJ. Elevated concentration of N-CAM VASE isoforms in schizophrenia. J Psychiatr Res 2000;34:25–34. [PubMed: 10696830]

Vawter MP, Usen N, Thatcher L, Ladenheim B, Zhang P, VanderPutten DM, Conant K, Herman MM, van Kammen DP, Sedvall G, Garver DL, Freed WJ. Characterization of human cleaved N-CAM and association with schizophrenia. Exp Neurol 2001;172:29–46. [PubMed: 11681838]

Viapiano MS, Matthews RT. From barriers to bridges: chondroitin sulfate proteoglycans in neuropathology. Trends Mol Med 2006;12:488–496. [PubMed: 16962376]

West MJ. Stereological methods for estimating the total number of neurons and synapses: issues of precision and bias. TINS 1999;22:51–61. [PubMed: 10092043]

Yamaguchi Y. Lecticans: organizers of the brain extracellular matrix. Cell Mol Life Sci 2000;57:276–289. [PubMed: 10766023]

Zacharias U, Rauch U. Competition and cooperation between tenascin-R, lecticans and contactin 1 regulate neurite growth and morphology. J Cell Sci 2006;119:3456–3466. [PubMed: 16899820]

Zhou XH, Brakebusch C, Matthies H, Oohashi T, Hirsch E, Moser M, Krug M, Seidenbecher CI, Boeckers TM, Rauch U, Buettner R, Gundelfinger ED, Fassler R. Neurocan is dispensable for brain development. Mol Cell Biol 2001;21:5970–5978. [PubMed: 11486035]

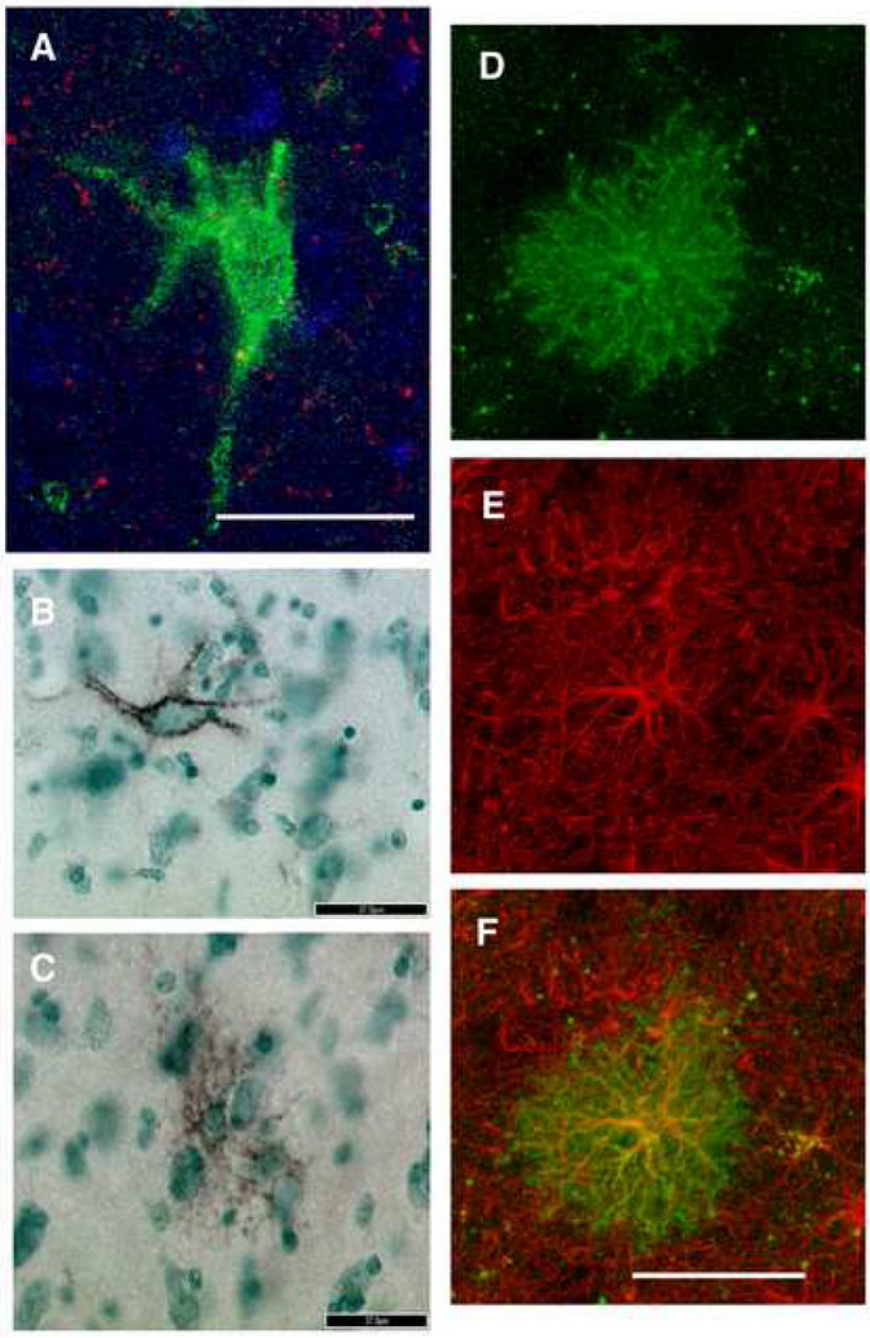

Figure 1. WFA-labeled perineuronal nets and glial cells in the human amygdala and co-labeling of WFA and GFAP

WFA lectin-histochemistry resulted in labeling of perineuronal nets (**A**, **B**) and glial cells (**C**, **D**) in the human amygdala. **A** and **B** represent confocal and light microscopy (DAB with methylgreen counterstaining) photomicrographs, respectively, of WFA-labeled perineuronal nets. Note the large size with respect to glial cells (**C**), the characteristic neuronal morphology and the hollow appearance. These characteristics contrast sharply with those of glial cells showing intracellular WFA-labeling, shown in **C** and **D** as light microscopy and confocal photomicrographs, respectively. These cells have small cell bodies and 'bushy', tightly packed, short processes. The large majority of WFA-labeled, putatively CSPG-expressing, glial cells

were also GFAP-immunoreactive. In **D**, **E**, and **F**, confocal photomicrographs of a glial cell labeled with WFA (**D,** green), GFAP (**E**, red) and the overlay of the markers (**F**, yellow). Scale bars are 50 μm **A**, **D**, **E**, and **F**; 37 μm **B**, **C**.

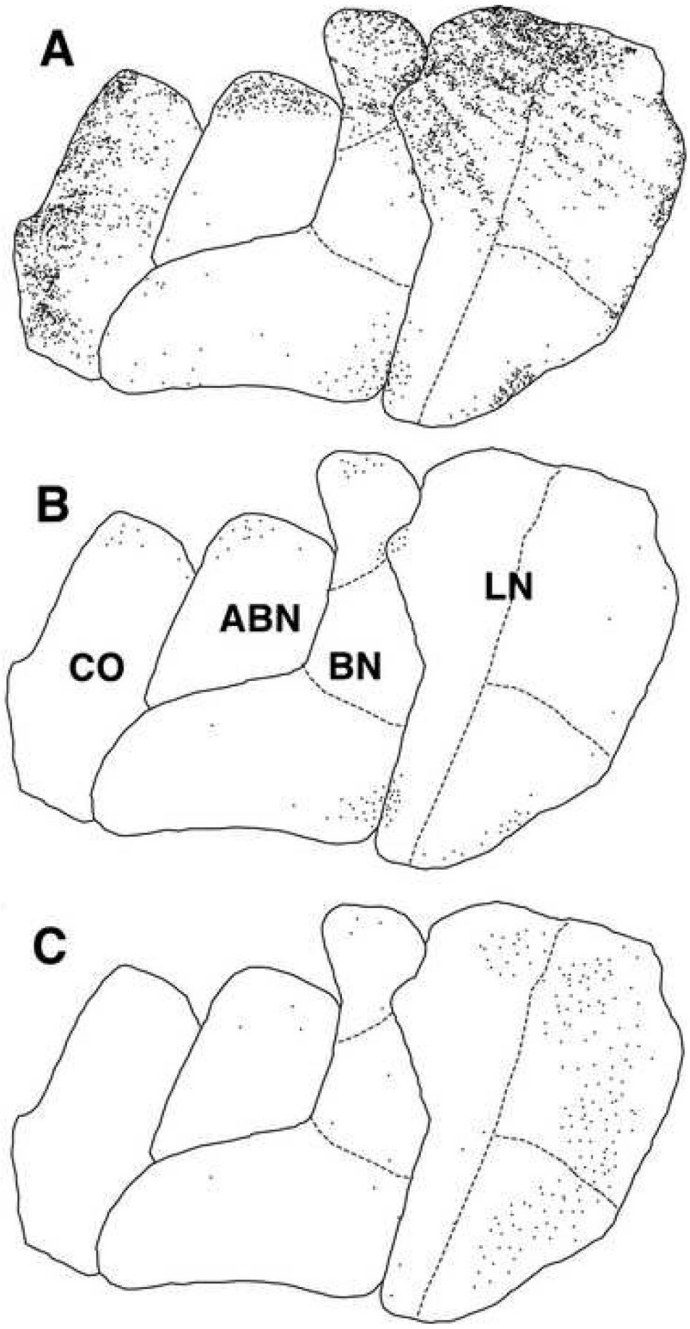

Figure 2. Glial cells expressing chondroitin sulfate proteoglycans may represent a subpopulation of astrocytes in the human amygdala

Schematic representation of the distribution of GFAP-immunoreactive cells (**A**), WFA-labeled glial cells (**B**), and WFA-labeled perineuronal nets (**C**) in the LN, BN, ABN and CO from one representative section of the amygdala in subject 14.

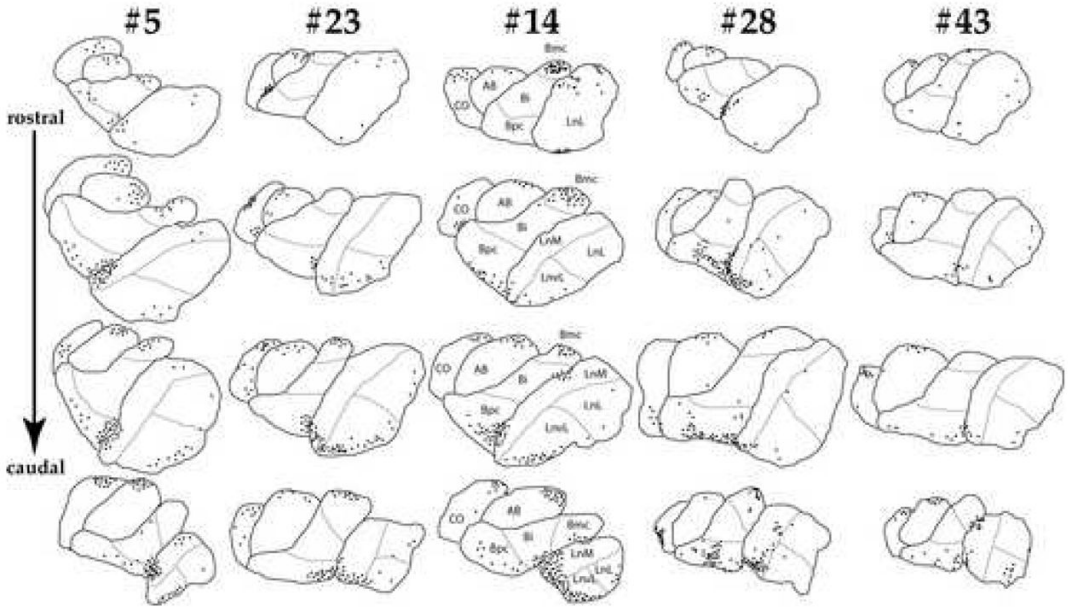

Figure 3. WFA-labeled glial cells show a consistent pattern of segregation within subregions of the human amygdala

Schematic representation of the distribution of WFA-labeled glial cells in four sections from the BLC-CO in subjects 5, 23, 14, 28, 43. The majority of these cells clustered between the medial LN and the parvicellular BN as well as along the ventral edge of these nuclei. Small cell clusters were also detected in the magnocellular BN and in the dorsal portion of the ABN and CO.

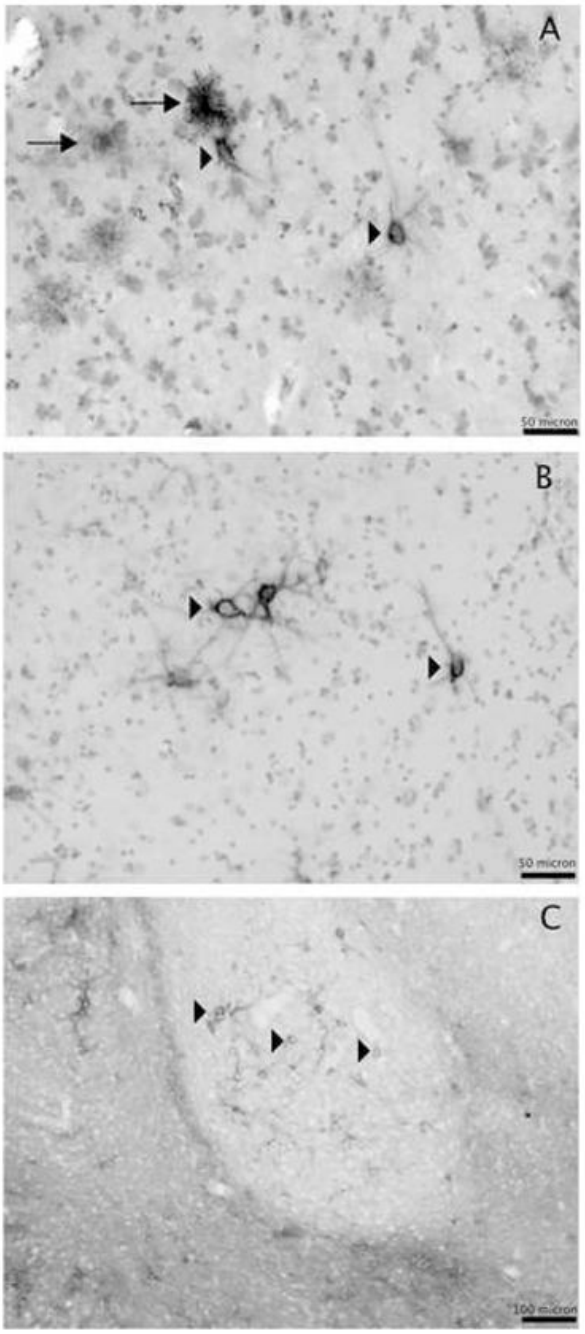

Figure 4. Intracellular WFA-labeling in glial cells was not detected in the rodent and nonhuman primate amygdala

Light microscopy photomicrographs showing WFA-labeled perineuronal nets (arrowheads) and glial cells (arrows) in the ventrolateral subdivision of the LN in human (**A**), WFA-labeled perineuronal nets (arrowheads) in the ventrolateral subdivision of the LN of a rhesus monkey (**B**) and in the BN of an adult (P60) rat (**C**). WFA labeled glial cells were not detected in the amygdala of rhesus monkeys and rats. Scale bars, **A, B** 50 μm; **C** 100 μm.

Table 1

Total numbers and numerical densities of WFA-labeled, putatively CSPG-expressing, glial cells in human BLC-CO.

	Total Number		Numerical Density	
Nucleus	**Mean**	**SD**	**Mean**	**SD**
LN	102,232	157,320	528.92	795.90
BN	52,832	68,882	396.47	608.95
AB	10,400	15,872	204.73	283.26
CO	13,104	11,656	455.40	469.60
BLC-CO	178,568	212,367	424.57	526.72

Numerical density is expressed as cells/mm^3

Table 2

Demographic and Descriptive Data of the Human Subject Cohort

code	Age (yr)	Gender	PMI (hr)	Cause of Death
5*	68	Female	14.8	Cardiac arrest
2	70	Male	23.2	Cardiac arrest
19	52	Male	32.1	Cardiac arrest
25	71	Male	24	Cardiac arrest
11	37	Male	18.8	Electrocution
31	65	Male	17.3	Cardiac arrest
21	53	Female	24	Melanoma
23*	62	Male	29.2	Cardiac arrest
36	70	Male	17.3	Abdominal aortic aneurysm
14*	58	Female	17.8	Carbon monoxide poisoning
16	72	Male	28.2	Cardiac arrest
35	74	Female	12.1	Cancer
28*	74	Male	15.8	Cardiac arrest
43*	85	Male	20.3	Cancer
8	78	Female	23.9	Cancer
	^65.9 ± 12.0	10M/5 F	^21.3 ±5.7	

* cases used for CSP-GFAP double labelling

^ mean ± standard deviation

Abbreviation: PMI, postmortem time interval